

Calculation of Stresses and Slips in Helical Layers of Dynamically Bent Flexible Pipes

J.-M. Leroy, P. Estrier

▶ **To cite this version:**

J.-M. Leroy, P. Estrier. Calculation of Stresses and Slips in Helical Layers of Dynamically Bent Flexible Pipes. Oil & Gas Science and Technology - Revue d'IFP Energies nouvelles, 2001, 56 (6), pp.545-554. 10.2516/ogst:2001044 . hal-02053964

HAL Id: hal-02053964
https://ifp.hal.science/hal-02053964

Submitted on 1 Mar 2019

HAL is a multi-disciplinary open access archive for the deposit and dissemination of scientific research documents, whether they are published or not. The documents may come from teaching and research institutions in France or abroad, or from public or private research centers.

L'archive ouverte pluridisciplinaire **HAL**, est destinée au dépôt et à la diffusion de documents scientifiques de niveau recherche, publiés ou non, émanant des établissements d'enseignement et de recherche français ou étrangers, des laboratoires publics ou privés.

Oil & Gas Science and Technology – Rev. IFP, Vol. 56 (2001), No. 6, pp. 545-554
Copyright © 2001, Éditions Technip

Calculation of Stresses and Slips in Helical Layers of Dynamically Bent Flexible Pipes

J.-M. Leroy[1] and P. Estrier[2]

1 Institut français du pétrole, 1 et 4, avenue de Bois-Préau, 92852 Rueil-Malmaison Cedex - France
2 Coflexip Stena Offshore, rue Jean-Hure, BP 7, 76580 Le Trait - France
e-mail: j-marc.leroy@ifp.fr - pascal.estrier@coflexip.fr

Résumé — Détermination des contraintes et déplacements des couches hélicoïdales des conduites flexibles soumises à des flexions dynamiques — Cet article présente une méthode de détermination des contraintes et des déplacements dans les couches hélicoïdales des pipelines flexibles lors de flexions dynamiques. Les déplacements de chacune des couches ne peuvent être déterminés indépendamment des autres couches à cause de la présence de frottement. Un couplage de la cinématique des couches est donc nécessaire. Une comparaison avec des mesures de déformations montre que les développements théoriques sont correctement validés.
Mots-clés : pipeline, flexible, flexion, déplacement, contrainte.

Abstract* — *Calculation of Stresses and Slips in Helical Layers of Dynamically Bent Flexible Pipes — *This paper deals with stress and displacement calculation in dynamically bent unbounded flexible pipes. The presented method is original in that movements and stresses of all helical layers are coupled. Good correlation between strain measurements and the theory has been found, and is shown in the paper.*
Keywords: flexible, pipe, bending, displacement, stress.

NOTATIONS

a	radius of a helical layer
C_b, C_n	transverse and normal curvatures of a curve
F_t, F_b, F_n	tangential, transverse and normal forces in a wire
M_t, M_b, M_n	tangential, transverse and normal moments in an wire
R	radius of curvature of the pipe
s	curvilinear abscissa along a helix
$\vec{t}$	unit tangential vector of a curve
$\vec{N}$	unit vector normal to the bent pipe
$\vec{B}$	unit transverse vector of a curve
x_1, x_2, x_3	rectangular coordinates of a point of a torus
α	initial laying angle of a helix
Δ_t, Δ_b	slip of a point of a helix relatively to the torus, respectively in $\vec{t}$ and $\vec{B}$ directions
$\varepsilon = \frac{a}{R}$	relative curvature of the pipe
θ, φ	angular coordinates of a point of a torus
Δ_p, Δ_c	slip of a point of a helix relatively to the torus, respectively along a parallel (θ constant), and along a meridian (φ constant)
$\frac{1}{\tau}$	torsion of a curve
σ	stress.

Subscripts

t	in tangential direction
b	in transverse direction.

Superscript

i	relative to the ith layer.

INTRODUCTION

Design life prediction of flexible risers is of outstanding importance to ensure reliability of offshore structures.

In a simplified manner, a flexible riser design is an iterative four-step procedure (Estrier, 1992):

- a first analysis gives the static behavior of the flexible pipe components under axial tension, internal and external pressure;
- a second analysis determines dynamic tension and curvature variations along the pipe according to environmental conditions (waves, current, vessel motions, etc.);
- a third analysis determines stresses and slips in pipe layers due to curvature variations;
- the last step uses the previous stresses to determine fatigue limits of the riser.

This paper deals with the third step, and mainly with tensile armour layers behavior that depend on time loading of the pipe.

The method is described in two steps. The first one is a geometrical analysis of deformed helices on a torus, where basic equations between curvatures and displacements are obtained. In the other one, friction and equilibrium equations are presented. A system of differential equations that links displacements and forces of helical layers is obtained. It is solved with a finite difference and a quasi Newton method.

Numerical examples of layers displacements and friction effects are then presented.

The paper ends with a comparison between theoretical results and strain measurements.

1 FLEXIBLE PIPE STRUCTURE

As shown on Figure 1, a flexible pipe used as a riser is typically made of the following layers (from inside to outside):

- a carcass, which is a metallic construction used to prevent, totally or partially, collapse of the internal sheath pipe due for example to external pressure;
- an internal sheath, which is an extruded polymer layer that ensures internal-fluid integrity;
- a pressure vault, which is a structural layer with a lay angle close to 90 degrees, and that increases the resistance of the pipe to internal and external pressure;
- tensile armour layers, which are structural layers with a lay angle typically between 20 and 55 degrees, and consist of helically wound wires. They are used to sustain tensile loads and internal pressure. Tensile armour layers are counter wound in pairs.
- anti-wear layers, which are nonmetallic extruded thermoplastic sheath or tape wrapping, used to minimize wear between structural layers,
- an outer sheath, which is an extruded polymer layer that protects pipe against penetration of sea water and external damages.

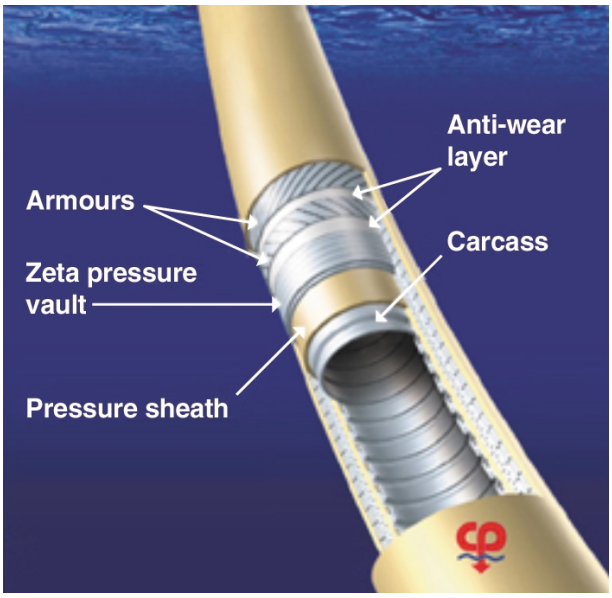


Figure 1

Example of flexible pipe.

Environmental conditions (waves, current, vessel motions, etc.), create variations in tension and curvatures of the riser and dynamic slips, stresses and friction forces in the previous layers.

The following method deals with the determination of these slips, stresses and friction forces, assuming that the time curvature of the pipe is given as explained by Estrier (Estrier, 1992).

2 GEOMETRICAL ANALYSIS

This first step gives basic relations between curvatures and displacements of deformed helices on a torus.

A curve on a surface can be defined in Darboux-Ribeaucourt axes $(\vec{t}, \vec{N}, \vec{B})$, where $\vec{t}$ is the unit tangential vector, $\vec{N}$ is the unit internal normal to the surface, $\vec{B} = \vec{t} \Lambda \vec{N}$ is in the transverse direction.

If s is the curvilinear abscissa along the curve, then:

$$\begin{bmatrix} \frac{d\vec{t}}{ds} \\ \frac{d\vec{N}}{ds} \\ \frac{d\vec{B}}{ds} \end{bmatrix} = \begin{bmatrix} 0 & C_n & C_b \\ -C_n & 0 & -\frac{1}{\tau} \\ -C_b & \frac{1}{\tau} & 0 \end{bmatrix} \begin{bmatrix} \vec{t} \\ \vec{N} \\ \vec{B} \end{bmatrix} \quad (1)$$

where C_b, C_n are respectively transverse and normal curvatures and $\frac{1}{\tau}$ is the torsion of the curve.

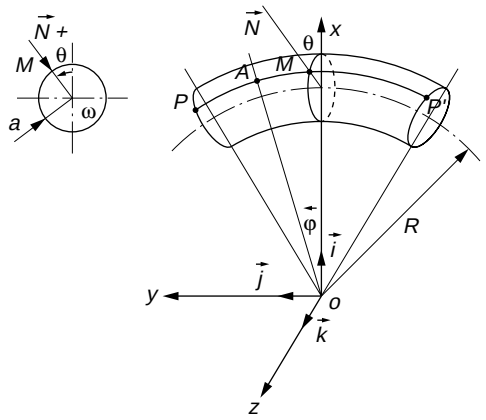


Figure 2

Mathematical parameters definition.

Assuming that the bent pipe is a torus of constant radius of curvature R and of radius a *(Fig. 2)*, a point M on the torus has the following coordinates in $(\vec{i}, \vec{j}, \vec{k})$ axes:

$$\begin{aligned} x_1 &= (R + a \cdot \cos\theta) \cdot \cos\varphi \\ x_2 &= (R + a \cdot \cos\theta) \cdot \sin\varphi \\ x_3 &= a \cdot \sin\theta \end{aligned} \tag{2}$$

As:

$$(ds)^2 = (dx_1)^2 + (dx_2)^2 + (dx_3)^2 \tag{3}$$

$$\vec{t} = \frac{dx_1}{ds}\vec{i} + \frac{dx_2}{ds}\vec{j} + \frac{dx_3}{ds}\vec{k} \tag{4}$$

$$\vec{N} = -\cos\theta \cdot \cos\varphi \cdot \vec{i} - \cos\theta \cdot \sin\varphi \cdot \vec{j} - \sin\theta \cdot \vec{k} \tag{5}$$

$\frac{ds}{d\theta}, C_b, C_n, \frac{1}{\tau}$ can be deduced from Equations (1) to (5):

$$\left(\frac{ds}{d\theta}\right)^2 = a^2 + R^2 \cdot v^2 \cdot g^2 \tag{6}$$

$$C_b = \left[\sin\theta \cdot (2 \cdot a^2 \cdot g + R^2 \cdot v^2 \cdot g^3) - a \cdot R \cdot v \cdot \frac{dg}{d\theta}\right]\left(\frac{d\theta}{ds}\right)^3 \tag{7}$$

$$C_n = \left[a + R \cdot v \cdot \cos\theta \cdot g^2\right]\left(\frac{d\theta}{ds}\right)^2 \tag{8}$$

$$\frac{1}{\tau} = R \cdot g \cdot \left(\frac{d\theta}{ds}\right)^2 \tag{9}$$

where:

$$g = \frac{d\varphi}{d\theta}, \varepsilon = \frac{a}{R}, v = 1 + \varepsilon \cdot \cos\theta$$

Hence curves on the torus are completely defined if (for example) $g = \frac{d\varphi}{d\theta}$ is given.

It is assumed that the deformed helices can be described by:

$$\frac{d\varphi}{d\theta} = \frac{\varepsilon}{tg\alpha}(1 + h(\theta, \varepsilon)) \tag{10}$$

where: $h(\theta, \varepsilon = 0) = 0$, α: initial laying angle of the helix.

The choice of Equation (10), applying far from end fittings and with a constant curvature of the pipe, was governed by previous studies of well-known curves on a surface, such as the geodesic or the loxodromic curves.

Introducing Equation (10) into Equations (6) to (8), the following results are obtained (refer to Appendix 1 for mathematical developments):

$$h = -\frac{1}{a\cos\alpha} \cdot \frac{d\Delta_b}{d\theta} \tag{11}$$

$$\gamma = \frac{\sin\alpha}{a}\frac{d\Delta_t}{d\theta} + \varepsilon \cdot \cos^2\alpha \cdot \cos\theta \tag{12}$$

$$\Delta C_n = \frac{\varepsilon}{a} \cdot \cos^2\alpha \cdot \left[(1 - 2\sin^2\alpha)\cos\theta - 2\frac{h}{\varepsilon}\sin^2\alpha\right] \tag{13}$$

$$\Delta C_b = \frac{\varepsilon}{a} \cdot \cos\alpha \cdot \left[(1 + \sin^2\alpha) \cdot \sin\theta - \frac{1}{\varepsilon}\frac{dh}{d\theta}\sin^2\alpha\right]$$

or: (14)

$$\Delta C_b = \frac{\varepsilon}{a} \cdot \cos\alpha \cdot (1 + \sin^2\alpha) \cdot \sin\theta + \frac{\sin^2\alpha}{a^2} \cdot \frac{d^2\Delta_b}{d\theta^2}$$

$$\Delta\frac{1}{\tau} = \frac{\varepsilon}{a} \cdot \cos\alpha \sin\alpha \cdot \left[-2\cos^2\alpha\cos\theta + (\sin^2\alpha - \cos^2\alpha)\frac{h}{\varepsilon}\right] \tag{15}$$

where:

Δ_t (respectively Δ_b) is the slip of a point of the helix relatively to the torus in the tangential (respectively transverse) direction;

γ is the tangential strain of the helix;

$\Delta\frac{1}{\tau}, \Delta C_b, \Delta C_n$ are variations of torsion, transverse and normal curvatures with respect to the undeformed straight pipe.

3 MECHANICAL ANALYSIS

The studied flexible pipe is made of n helical layers of laying angle α^i (i = 1 to n). The internal layer is supported by a substrate that is modeled as a cylinder. We define:

R the constant radius of curvature of the bent substrate;

a^i the radius of the *ith* helical layer;

$\vec{q}_n^i$ the normal force (per unit length of a helix) at the lower interface of the helical layer;

$\vec{q}_f^i$ the friction force (per unit length of a helix) at the lower interface of the helical layer;

f^i the friction coefficient on the lower interface of the *ith* helical layer.

Subscripts *t* and *b* will be used to refer to the tangential and transverse directions. For example: $q_{f,t}^i = \vec{q}_f^i \cdot \vec{t}^{\,i}$.

Note that the slip of the i^{th} helical layer relatively to layer $i-1$ is defined as $\vec{\delta}^i$, with:

$$\begin{aligned}\delta_b^i &= \vec{\delta}^i \cdot \vec{B}^i \\ &= \Delta_b^i - \Delta_b^{i-1} \cdot \cos(\alpha^i - \alpha^{i-1}) - \Delta_t^{i-1} \cdot \sin(\alpha^{i-1} - \alpha^i) \\ \delta_t^i &= \vec{\delta}^i \cdot \vec{t}^{\,i} \\ &= \Delta_t^i - \Delta_b^{i-1} \cdot \sin(\alpha^i - \alpha^{i-1}) - \Delta_t^{i-1} \cdot \cos(\alpha^i - \alpha^{i-1})\end{aligned} \tag{16}$$

3.1 Equations of Friction

When sliding occurs, friction forces are opposed to the sliding direction (or sliding velocity). At a given point of the internal helical layer ($i = 1$), equations of friction can be written as:

$$q_{f,t}^1 = \vec{q}_f^1 \cdot \vec{t}_1 = -\frac{\dot{\Delta}_t^1}{\sqrt{\beta^2 + \left(\dot{\Delta}_t^1\right)^2 + \left(\dot{\Delta}_b^1\right)^2}} \cdot f^1 \cdot q_n^1 \tag{17}$$

$$q_{f,b}^1 = \vec{q}_f^1 \cdot \vec{b}_1 = -\frac{\dot{\Delta}_b^1}{\sqrt{\beta^2 + \left(\dot{\Delta}_t^1\right)^2 + \left(\dot{\Delta}_b^1\right)^2}} \cdot f^1 \cdot q_n^1 \tag{18}$$

and, for layers 2 to *n*:

$$q_{f,t}^i = \vec{q}_f^i \cdot \vec{t}_i = -\frac{\dot{\delta}_t^i}{\sqrt{\beta^2 + \left(\dot{\delta}_t^i\right)^2 + \left(\dot{\delta}_b^i\right)^2}} \cdot f^i \cdot q_n^i \tag{19}$$

$$q_{f,b}^i = \vec{q}_f^i \cdot \vec{b}_i = -\frac{\dot{\delta}_b^i}{\sqrt{\beta^2 + \left(\dot{\delta}_t^i\right)^2 + \left(\dot{\delta}_b^i\right)^2}} \cdot f^i \cdot q_n^i \tag{20}$$

where:

$$\dot{\Delta}_t^1 = \frac{\partial \Delta_t^1}{\partial \varepsilon}, \dot{\Delta}_b^1 = \frac{\partial \Delta_b^1}{\partial \varepsilon}$$

are sliding velocities of the first layer on the substrate, and

$$\dot{\delta}_t^i = \frac{\partial \delta_t^i}{\partial \varepsilon}, \dot{\delta}_b^i = \frac{\partial \delta_b^i}{\partial \varepsilon}$$

are sliding velocities of the layer *i* ($i > 1$) relatively to layer $i-1$.

The parameter β is a coefficient to avoid numerical problems when sliding velocities are null, *i.e.* when surfaces are stuck. Equations of friction as presented above are then appropriate when sliding or sticking phenomena occur.

3.2 Equilibrium Equations

Equilibrium of a length ds of a helix of the ith layer, submitted to internal force $\vec{F}^i$ and moment $\vec{M}^i$, and external friction and normal forces $\vec{q}_n^i ds$, $\vec{q}_n^{i+1} ds$, $\vec{q}_f^i ds$ and $\vec{q}_f^{i+1} ds$ on his lower and upper interfaces, gives, in $\vec{t}_i, \vec{N}_i, \vec{b}_i$ directions:

$$\begin{aligned}&\frac{dF_t^i}{ds} - F_b^i C_b^i - F_n^i C_n^i + q_{f,t}^i \ldots \\ &\quad \ldots - q_{f,t}^{i+1} \cos(\alpha^{i+1} - \alpha^i) - q_{f,b}^{i+1} \sin(\alpha^i - \alpha^{i+1}) = 0\end{aligned} \tag{21}$$

$$F_t^i C_n^i + \frac{1}{\tau_n^i} F_b^i + \frac{dF_n^i}{ds} - q_n^i + q_n^{i+1} = 0 \tag{22}$$

$$\begin{aligned}&F_t^i C_b^i + \frac{dF_b^i}{ds} - \frac{1}{\tau_n^i} F_n^i + q_{b,t}^i \ldots \\ &\quad \ldots - q_{f,t}^{i+1} \sin(\alpha^{i+1} - \alpha^i) - q_{b,t}^{i+1} \cos(\alpha^{i+1} - \alpha^i) = 0\end{aligned} \tag{23}$$

$$\frac{dM_t^i}{ds} - M_b^i C_b^i - M_n^i C_n^i = 0 \tag{24}$$

$$M_t^i C_n^i + \frac{1}{\tau_n^i} M_b^i + \frac{dM_n^i}{ds} - F_b^i = 0 \tag{25}$$

$$M_t^i C_b^i + \frac{dM_b^i}{ds} - \frac{1}{\tau_n^i} M_n^i + F_n^i = 0 \tag{26}$$

Note that, for the external layer ($i = n$):

$$q_n^{i+1} = 0, q_{f,t}^{i+1} = 0, q_{f,b}^{i+1} = 0$$

if friction on the external sheath is neglected.

3.3 Constitutive Equations

The behavior of helices are given by:

$$F_t^i = E^i A^i \gamma^i \tag{27}$$

$$M_t^i = -G^i I_p^i \Delta \frac{1}{\tau_n^i} \tag{28}$$

$$M_b^i = E^i I_n^i \Delta C_n^i \tag{29}$$

$$M_n^i = -E^i I_b^i \Delta C_b^i \tag{30}$$

with $E^i, A^i, I_p^i, I_n^i, I_b^i$ respectively the Young's modulus, the section, and torsional, normal and transverse inertia of the helix.

It is here assumed that the normal principal axis of the wire is the same than the normal to the surface $\vec{N}$.

3.4 Resolution

The nonlinear problem is solved with the finite difference method.

It is first assumed that all wires of a given layer have the same behavior. Then, only one wire of each layer is partitioned into n_p intervals of length $\Delta\theta = \frac{2\pi}{n_p}$, with $n_p + 1$ points x_k^i initially positioned at:

$$\theta_k^i = (k-1)\Delta\theta \text{ if } \alpha^i > 0$$

$$\theta_k^i = 2\pi - (k-1)\Delta\theta \text{ if } \alpha^i < 0 \; (k = 1 \text{ to } n_p + 1)$$

The given dynamic relative curvature of the pipe is also partitioned into n_ε intervals of length $\Delta\varepsilon$.

From finite difference method, the following approximation, for any function $u(\theta, \varepsilon)$ is used:

$$\frac{\partial u(\theta,\varepsilon)}{\partial\theta} = \frac{u(\theta+\Delta\theta,\varepsilon) - u(\theta-\Delta\theta,\varepsilon)}{2\Delta\theta}$$

$$\frac{\partial^2 u(\theta,\varepsilon)}{\partial\theta^2} = \frac{u(\theta+\Delta\theta,\varepsilon) - 2u(\theta,\varepsilon) + u(\theta-\Delta\theta,\varepsilon)}{\Delta\theta^2}$$

$$\frac{\partial u(\theta,\varepsilon)}{\partial\varepsilon} = \frac{u(\theta,\varepsilon) - u(\theta,\varepsilon-\Delta\varepsilon)}{\Delta\varepsilon}$$

In order to reduce time calculation, chosen unknowns in the resolution are the transverse and tangential displacements $\Delta_t^i(\theta_k), \Delta_b^i(\theta_k)$, with k = 1 to $n_p + 1$ and i = 1 to n. The problem size is then $2n\,(n_p + 1)$ unknowns.

It is considered also that relative displacements are small, so a given point x_k^i is always in contact with the same points x_k^{i-1} and x_k^{i+1} of the upper and lower layers.

Giving a curvature ε and a step $\Delta\varepsilon$, Equations (21) and (23) are the solved equations at points x_k^i, $k \neq 1$, $k \neq n_p + 1$, i = 1 to n. For k = 1, $k = n_p + 1$, the following boundary conditions are used: $\Delta_t^i(\theta_k) = 0$, $\Delta_b^i(\theta_k) = 0$ (i = 1 to n). The solution is determined with a quasi Newton method.

Equations (12) to (15), (17) and (18) (or (19) and (20)), (22) and (25) to (30), give the relations between

$$F_t^i, F_n^i, F_b^i, M_t^i, M_n^i, M_b^i, \Delta\frac{1}{\tau_n^i}, \Delta C_n^i, \Delta C_b^i, \gamma^i, q_n^i, q_{f,t}^i, q_{f,b}^i$$

and the unknowns $\Delta_t^i(\theta_k)$, $\Delta_b^i(\theta_k)$.

Initially (straight pipe, $\varepsilon = 0$), $\Delta_t^i(\theta_k) = 0$, $\Delta_b^i(\theta_k)$ for i = 1 to n and k = 1 to $n_p + 1$.

4 THEORETICAL EXAMPLES

In this section, a flexible pipe is subjected to cycles of curvature from $\frac{1}{R} = 0$ to $\frac{1}{R} = 0.1\ \text{m}^{-1}$. It is made of two armour layers.

Input data are the following:

$a^1 = 78.3$ mm, $a^2 = 83.8$ mm

$\alpha^1 = -35°$, $\alpha^2 = 35°$

$A^1 = A^2 = 36\ \text{mm}^2$

$E^1 = E^2 = 2 \cdot 10^{11}$ Pa

initial tangential forces due to a traction of 500 kN are $F_t^1 = 7500$ N, $F_t^2 = 6300$ N.

Twenty cycles of bending are simulated. A coefficient of friction equal to 0.15 is used for all interfaces (between the internal armour layer and the substrate, and between both armour layers).

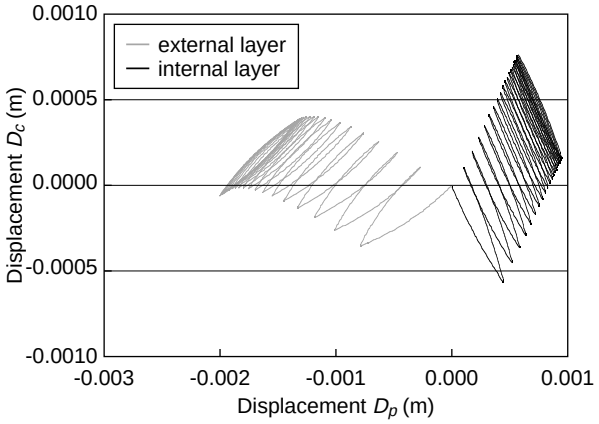


Figure 3

Trajectories of armour layers (Δ_c versus Δ_p for the internal helix, δ_c versus δ_p for the external helix) in cycles of curvature ($\theta = \frac{\pi}{2}$).

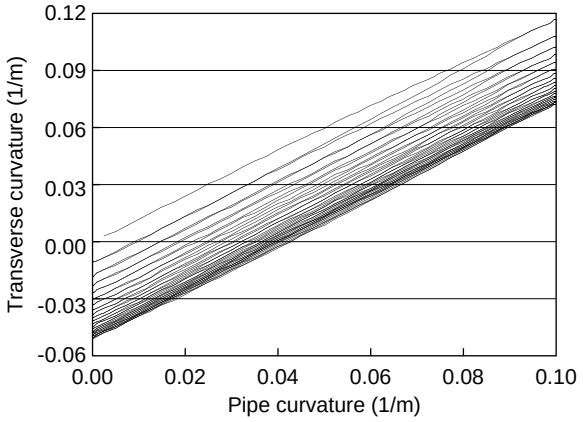


Figure 4

Transverse curvature of the internal armour layer in cycles of curvature ($\theta = \frac{\pi}{2}$).

Displacements (Δ_c versus Δ_p for the internal helix, δ_c versus δ_p for the external helix) and transverse curvatures ΔC_b of internal and external helices are represented in Figures 3, 4 and 5 on neutral bending axis ($\theta = \frac{\pi}{2}$) as a function of pipe curvature. These figures point out that a steady cycle of movement is obtained for each helix after only a few cycles of variation of curvature of the pipe. Steady cycles occur around geodesic curves and are centered on half the amplitude of geodesic displacements. The number of cycles necessary to reach the steady state depends on friction.

Figure 6 shows axial stress on extrados and intrados of internal and external helices versus the pipe curvature. Friction hysteretic effect is clearly shown.

Figures 7 to 14 show displacements, curvatures and stresses along internal and external helices, for minimum ($\frac{1}{R}$ = 0) and maximum ($\frac{1}{R}$ = 0.1 m^{-1}) curvatures of the pipe, for the first and 20th cycles of curvature. These figures show that variations of tangential displacements and stresses with cycles of curvature are small compared to variations of transverses displacements and curvatures. These figures show also that, after a few cycles of pipe curvatures, all displacements and curvatures have sinusoidal (or cosinusoidal) shapes versus θ, and tangential stresses have globally linear shapes. These shapes can be used to simplify the resolution, as was done in a previous work (Féret *et al.*, 1995).

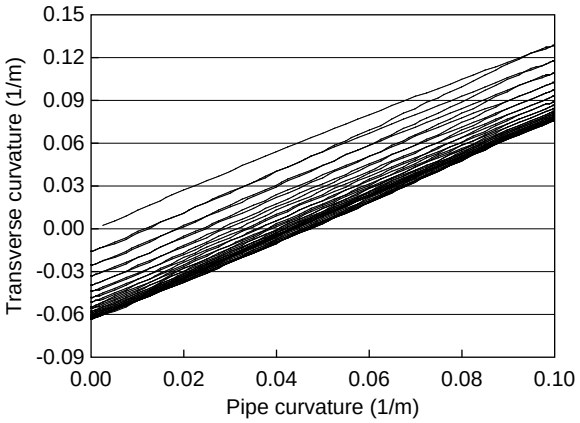


Figure 5
Transverse curvature of the external armour layer in cycles of curvature ($\theta = \frac{\pi}{2}$).

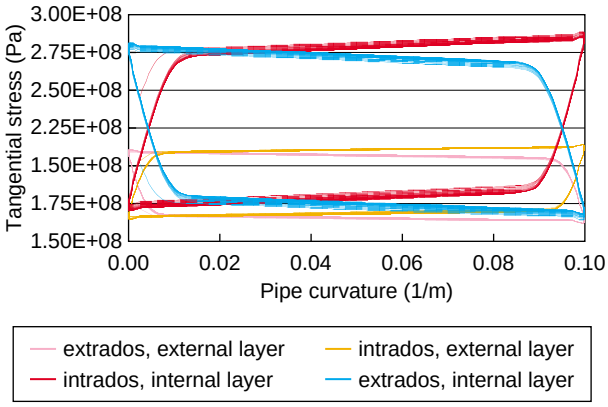


Figure 6
Axial stress of armour layers in cycles of curvature.

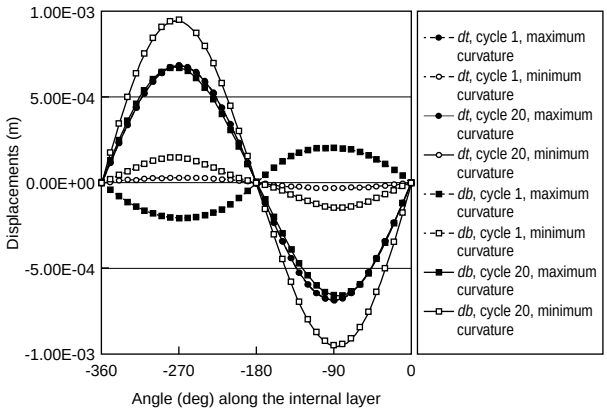


Figure 7
Displacements Δ_t and Δ_b along the internal armour layer.

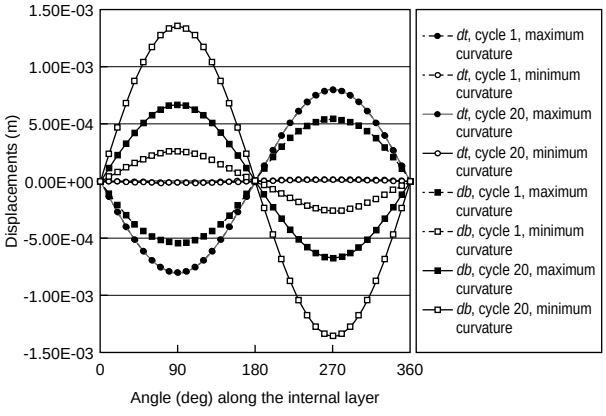


Figure 8
Displacements Δ_t and Δ_b along the external armour layer.

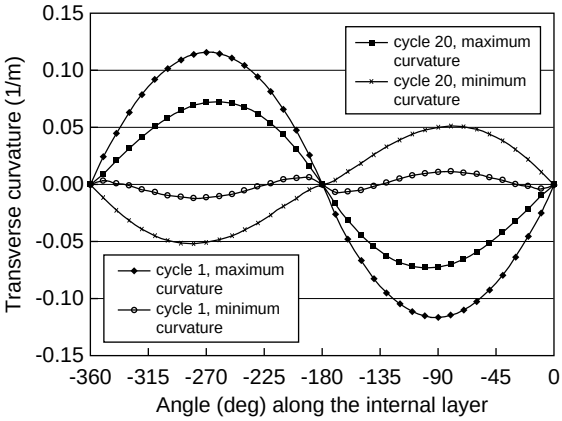


Figure 9

Transverse curvature along the internal armour layer.

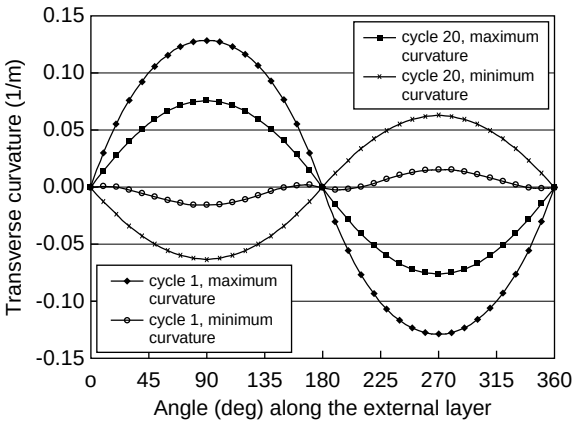


Figure 10

Transverse curvature along the external armour layer.

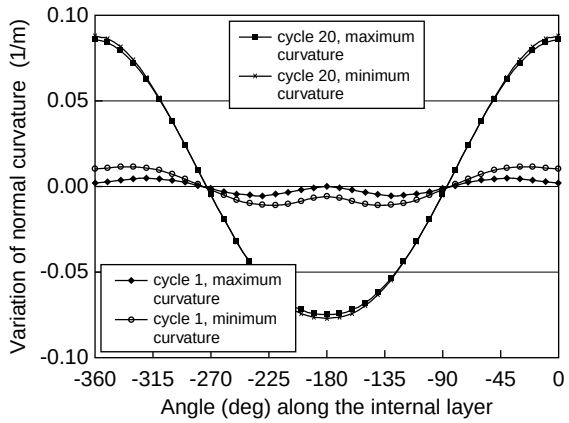


Figure 11

Normal curvature along the internal armour layer.

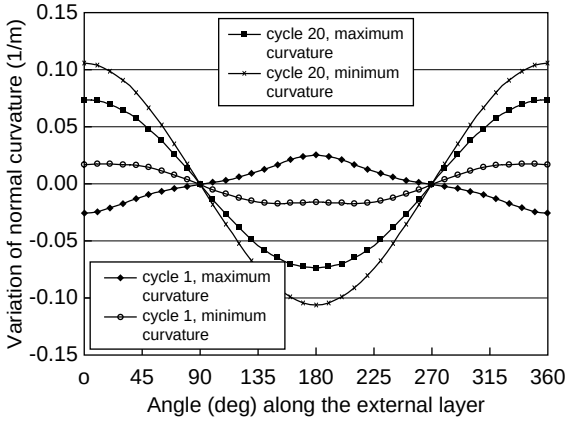


Figure 12

Normal curvature along the external armour layer.

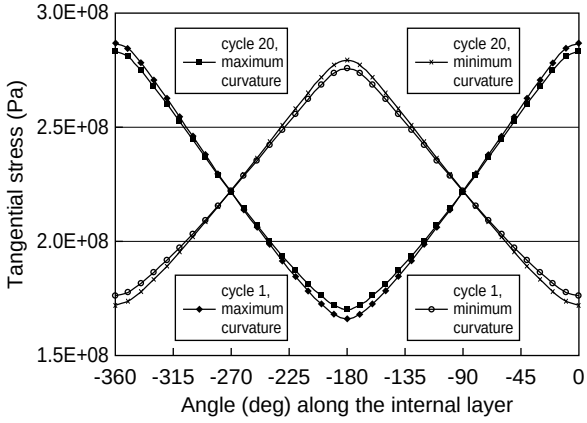


Figure 13

Axial stress along the internal armour layer.

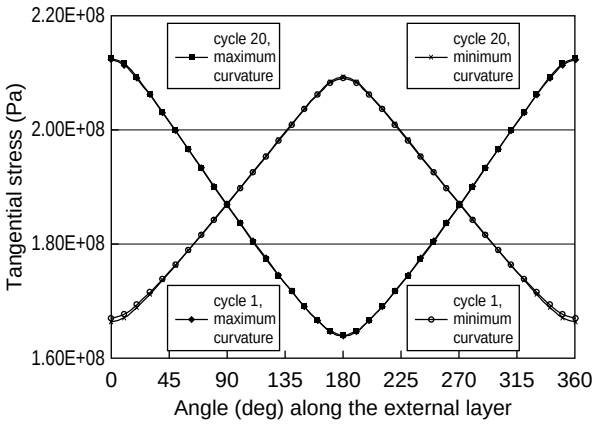


Figure 14

Axial stress along the external armour layer.

Theory-Experiments Comparison

A 4" internal diameter *Coflexip* flexible pipe of 8 m in length was tested on a dynamic bench test located at *IFP*. Both end-fittings of the flexible pipe can rotate and one end-fitting can translate *(see Fig. 15)*. Imposed rotations and translation were chosen to obtain (as far as possible) constant variations of curvature along the pipe.

Windows were cut in the external sheath at the pipe center and strain gauges were stuck on the external helical layer, at $\theta = 0$ (extrados), $\theta = \frac{\pi}{2}$ (neutral bending axis) and $\theta = \pi$ (intrados). Parallel strain gauges were used to obtain both axial and transverse strain variations. In each window, three gauges were stuck on adjacent armours (strain gages number 1 to 3 at intrados, number 4 to 6 on the neutral bending axis, and number 7 to 9 at extrados).

Test results presented here were obtained with an internal pressure of 40 MPa and a variation of pipe curvature equal to $\Delta \frac{1}{R} \cong 0.09\ m^{-1}$. Figures 16 to 18 show experimental results and the dispersion can than be found in flexible pipes.

Note that the pipe has an anti-wear layer between two armour layers. These three layers were modeled.

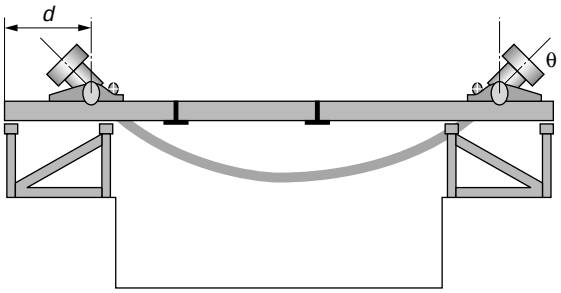


Figure 15

Dynamic bench test.

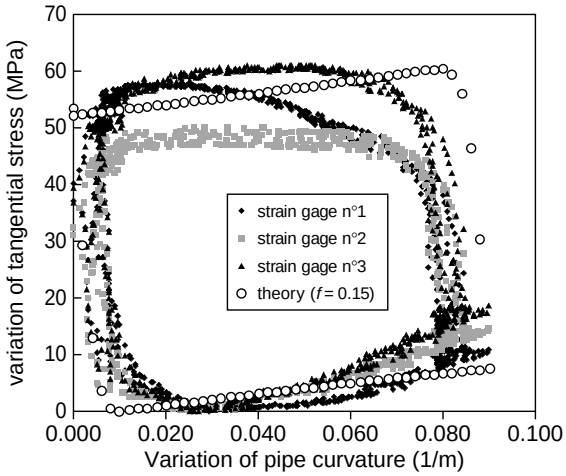


Figure 16

Theoretical and measured tangential stresses at intrados.

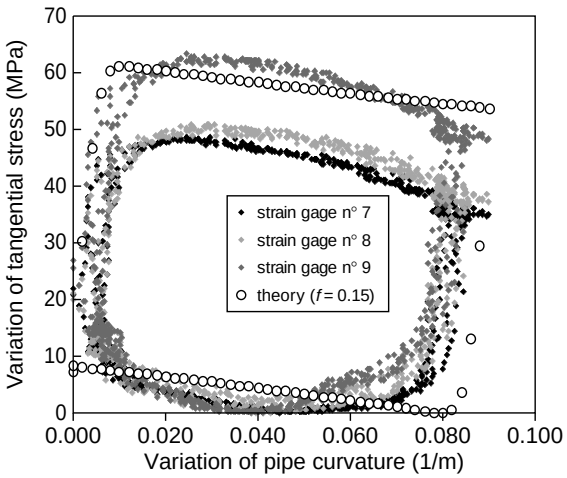


Figure 17

Theoretical and measured tangential stresses at extrados.

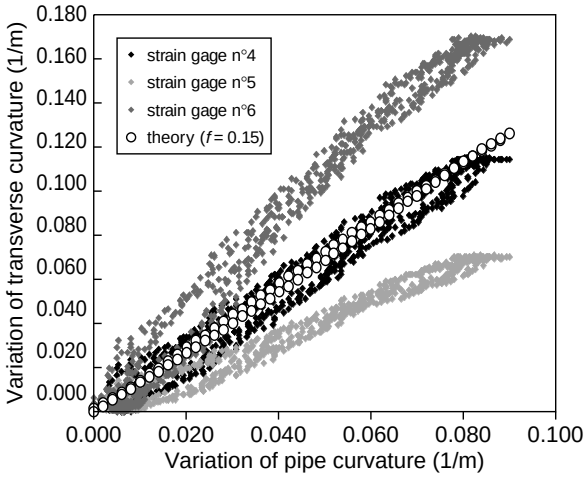


Figure 18

Theoretical and measured transverse curvatures at neutral bending axis.

Theoretical results were obtained as following:

- initial forces F_t due to pressure were determined with dedicated computer program (Féret and Momplot, 1989);
- experimental data (tangential strain) at extrados and intrados, were used to determine the friction coefficient. A value of 0.15 was obtained, as shown in Figures 16 and 18;
- measured pipe curvature variations on the bench test were used in theoretical simulations.

Theoretical and experimental variations of axial stress ($\theta = 0$ or $\theta = \pi$) and transverse bending stress ($\theta = \frac{\pi}{2}$) were compared, both in variations and in shapes.

Figures 16 to 18 show that shapes of both axial and transverse strain variations are well predicted by theory, and that the relative error do not exceed 30%.

The presented theory is then in good agreement with experimental measurements.

CONCLUSION

A method of dynamic stress and displacement calculation in flexible pipelines has been presented. It is based on geometrical, friction and equilibrium equations in helical layers. Good correlation has been found with strain measurements.

REFERENCES

Estrier, P. (1992) Updated Method for the Determination of the Service Life of Flexible Risers. *Proceedings of the First European Conference Marinflex*.

Féret, J. and Momplot, G. (1989) Caflex, Computer Program for Capacity Analysis of Flexible pipes. *IFP - SINTEF Structural Engineering Report*, No. STF71 F91019.

Féret, J., Leroy, J.M. and Estrier, P. (1995) Calculation of Stresses and Slips in Flexible Armour Layers with Layers Interaction. *ASME, Proceedings of the 14th International Conference on Offshore Mechanics and Artic Engineering*, **V**, 469-474.

Final manuscript received in October 2001

APPENDIX 1

When neglecting terms in ε^2, ε^3, ...:

$$\left(\frac{ds}{d\theta}\right)^2 = a^2 + R^2 \cdot v^2 \cdot g^2 \quad \text{and} \quad g = \frac{d\varphi}{d\theta} = \frac{\varepsilon}{tg\alpha}(1 + h(\theta, \varepsilon))$$

give:

$$\frac{ds}{d\theta} = \frac{a}{\sin\alpha}\left[1 + \cos^2\alpha(\varepsilon \cdot \cos\theta + h)\right]$$

If a point M is located with

$$\theta = \theta_0, s = s_0 = \frac{a\theta_0}{\sin\alpha}$$

when $\varepsilon = 0$ (straight pipe) and $\theta = \theta_\varepsilon$, $s = s_\varepsilon$ when $\varepsilon \neq 0$ (bent pipe), let introduce Δ_p the displacement of M (relatively to the torus) along a parallel (θ constant), and Δ_c the displacement along a meridian (φ constant):

$$\Delta_c = a \cdot (\theta_\varepsilon - \theta_0), \Delta_p = (R + a \cdot \cos\theta)\left[\int_0^{\theta_\varepsilon} \frac{d\varphi}{d\theta} d\theta - \frac{\varepsilon\theta_0}{tg\alpha}\right]$$

It is then found that:

$$h = \frac{1}{a}\left(tg\alpha \frac{d\Delta_p}{d\theta} - \frac{d\Delta_c}{d\theta}\right)$$

As:

$$\Delta_b = \Delta_c \cos\alpha - \Delta_p \sin\alpha: \quad h = -\frac{1}{a\cos\alpha}\frac{d\Delta_b}{d\theta}$$

To get γ the tangential strain of the helix, we use:

$$\int_0^{\theta_\varepsilon} \gamma \frac{ds}{d\theta} d\theta = s_\varepsilon - s_0 = \int_0^{\theta_\varepsilon} \frac{ds}{d\theta} d\theta - \frac{a\theta_0}{\sin\alpha}$$

$$= \int_0^{\theta_\varepsilon} \frac{a}{\sin\alpha}\left[1 + \cos^2\alpha(\varepsilon \cdot \cos\theta + h)\right] d\theta - \frac{a\theta_0}{\sin\alpha}$$

so:

$$s_\varepsilon = s_0 + \Delta_t + \frac{a}{\sin\alpha}\cos^2\alpha \cdot \varepsilon \cdot \sin\theta$$

$$\gamma \frac{ds}{d\theta} = \frac{d}{d\theta}(s_\varepsilon - s_0) = \frac{\sin\alpha}{a}\frac{d\Delta_t}{d\theta} + \cos^2\alpha \cdot \varepsilon \cdot \cos\theta$$